Applied Mathematics and Computation 232 (2014) 1151–1165

Contents lists available at ScienceDirect

Applied Mathematics and Computation

journal homepage: www.elsevier.com/locate/amc

Using detection of vehicular presence to estimate shockwave speed and upstream traffics for a signalized intersection

Hsun-Jung Cho [a,*], Ming-Te Tseng [b], Ming-Chorng Hwang [c]

[a] Department of Transportation Technology and Management, National Chiao Tung University, Hsinchu 300, Taiwan
[b] Chien-Chen Technology Corporation, No.79, Hsien Cheng 16th Street, Chupei, Hsinchu 302, Taiwan
[c] Microelectronics and Information Systems Research Center, National Chiao Tung University, Hsinchu 300, Taiwan

ARTICLE INFO

Keywords:
Shockwave speed
LWR traffic flow theory
Signal control
Vehicle detection

ABSTRACT

Based on the Lighthill–Whitham–Richards (LWR) traffic flow theory, this paper provides alternative methods to compute shockwave speed mainly by using detection data that reflects three states of vehicular presences: vehicles in moving, vehicles stopped, and void of vehicles. As the duration of a state is firmly identified within a cycle, the proposed methods compute shockwave speeds directly by means of Euclidian geometrics on time–space trajectory of shockwaves. This approach is also applicable to congested signal links with a long queue (but a residual queue) beyond detection zone. In addition, given signal timing and the shockwave speeds calculated by the methods, characteristics of arrival traffics, i.e. upstream flow rate and speed, can be predicted before the end of current cycle. It justifies that the methods are capable of whether to extend green phase before next cycle or not and will be a promising tool for real-time operations of signal control. Finally, the predicted shockwave speeds, upstream flow rate, and space mean speed by the proposed method are testified using simulated data from CORSIM. The mean absolute percentage errors of the estimated speeds of forward recovery shockwave and backward forming shockwave are 4.0% and 12.4% respectively. For the predicted flow rate and space mean speed of downstream arrival traffics, the mean absolute percentage errors are 18% and 4%, respectively. The results demonstrate the effectiveness of the presented approach.

1. Introduction

A traffic signal, like a switch, built at an intersection conducts passing traffics when to go and when to stop alternatively. Such an operation at signalized approaches causes cyclic change of queuing phases, both accumulating and discharging processes, that begins from stop line and proceeds to upstream. Oversaturation takes place at urban signal links frequently over peak hours. As defined conceptually, it reveals traffic queues being unable to disperse fully during a cycle either due to not enough green time or because of downstream blockage when traffic demand exceeds the capacity of signalized intersection. How to estimate oversaturated queues effectively by real-time data from detectors is an important research issue on solving the congestion problem of city traffics. Most existing studies evaluate signal queues mainly relying on traffic volumes, speed and occupancies observed from surveillance systems no matter shockwave theory or queuing models applied. However, vehicle detectors usually fail to provide such data in peak periods because stopped vehicles occupy detection zone. This

* Corresponding author.
E-mail addresses: hjcho001@gmail.com (H.-J. Cho), odder@cct.com.tw (M.-T. Tseng), mchwang1966@nctu.edu.tw (M.-C. Hwang).

http://dx.doi.org/10.1016/j.amc.2013.12.180
0096-3003/

paper concentrates on the subject of how to determine shockwave speed on congested arterials by using detection of vehicular presence but not by that of traffic volumes, speed and occupancies. The discussed shockwave structure also follows the Lighthill–Whitham–Richards (LWR) traffic flow theory [12,18]. As the detection of vehicle presence can be clearly identified, the proposed methods calculate shockwave speeds by employing Euclidian geometrics on the time–space diagram of shockwave propagations. The following paragraphs are a brief review on shockwave theory based studies and end with remarks on their limitations.

The application of wave behavior to traffic study was first presented independently by Lighthill and Whitham in 1955 and Richards in 1956. Shockwave structure derived from LWR traffic flow theory was widely applied to describe queue dynamics and performance measures for a signalized intersection. These two classic works also provided a preliminary attempt to how the theory might be utilized to describe traffics at road junctions. Michalopoulos et al. [16] formally extended the shockwave theory to the case at signalized links. The approach is macroscopic in nature and considers interrupted traffic as a continuum fluid to demonstrate the shockwave propagation and the evolution of queue periodically downstream of a traffic signal. Stephanopoulos et al. [15] and Michalopoulos et al. [17] formulated the dynamics of formation and dissipation of queues at isolated signalized intersections by solving the conservation equations along the street. The studies also developed a real-time control policy by minimizing total intersection delays subject to queue length constraints. However, these theoretic models consume full information of arrival traffics that limits their empirical applications to conditions with perfect detection data. We will rearrange shockwave speed equations in Section 2 with the assumed flow-density curve in a specific style. It forms an introductory material that is insightful for the proposed methods to compute shockwave speeds without such restrictions. For other notable reviews of shockwave-related traffic flow theories, we refer to [20,9,11,14,6,7]. Following the shockwave terminology used in [14], a typical illustration of multiple shockwaves at a signalized approach is show in Fig. 1 with dimensions both in time and space. Vehicle tracks are indicated in thin lines and shockwaves in boldface. As red light on, vehicles are forced to stop, that forms a backward forming shockwave, the line segment $\overline{AEG}$ for example, moving upstream of the approach. At the end time of red light, vehicles begin to release in a maximal flow rate, or saturation flow rate, generating a backward recovery shockwave, e.g. $\overline{BG}$. If the two shockwaves meets as shown at point *G* in Fig. 1, a third shockwave, a forward recovery shockwave, such as $\overline{GD}$, is actuated simultaneously. The subsequent queues within a cycle can be obviously observed, e.g. $\overline{BF}$ and $\overline{CG}$. The total stopped delay for through vehicles is assessed by adding up the area of zone *AEGB*.

There are still many studies making use of shockwave analysis in interrupted traffic flow propagation and queuing problem [2]; in stopped delay measurement [1]; in phase time determination [3,5]; and in forecasting traffic system performance [8,19]. These studies were used to determine shockwave speeds by means of traffic volume, speed, and density [10,17,1,5]. In particular, a serial field studies have been conducted based on the SMART-SIGNAL system on arterials in the Twin Cities. By exploiting high-resolution "event-based" traffic signal data (including both vehicle-detector actuation events and signal phase change events), the serial studies make considerable progress on estimation of long queues [13], on identification of oversaturated intersections by quantifying temporally and spatially the detrimental effects of oversaturation on signal operations with the oversaturation severity index [22], on developing a stable trapezoidal form of the cycle-based arterial fundamental diagram [21], and to renew interrupted traffic flow analysis by the shockwave profile model [23].

However, the above studies have two types of limitations. The first one, shockwave speeds estimated using conventional traffic data by detectors, e.g. volume, headway, and occupancy, are less accurate when traffics in bumper-to-bumper. It is because detectors usually operate inaccurately under heavily congested circumstance. Upstream arrival rate can not be predicted before next cycle is the second deficiency occurred in previous investigations. In order to make further developments from them, Cho and Tseng [4] delivered a rudimentary idea to detect only backward forming shockwave under oversaturated traffics with a fixed phase time. This paper improves the method in [4] and extends to forecast upstream flow rate by the presence of vehicle that remains accurate even under oversaturated condition. Contributions of this paper mainly relies on: (1) expanding the results of [4] on applicability at signalized intersections in terms of calculating more shockwaves speeds and dynamic signal timing considered, (2) the capability of computing extra green time to discharge traffic queue before the end of a cycle, and (3) the development of a method to forecast upstream flow beyond detection zone.

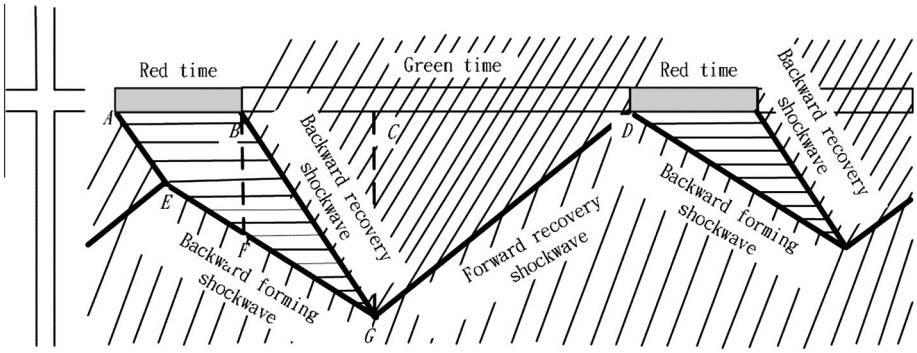

Fig. 1. Shockwaves in the time–space domain for a signalized intersection.

The following paragraphs of this paper are organized as follows. Model formulations describing detection of shockwaves are presented in Section 2. The results of proposed methods are numerically testified in several simulation scenarios on CORSIM and deeply discussed in Section 3. Section 4 concludes this paper with some remarks.

2. Formulation

The formulation section comprises five parts. Section 2.1 describes the structure among shockwaves, speeds, and flows. The traffic parameters, stopped duration, moving duration, and empty duration, are defined in Section 2.2. In Section 2.3, detection of the shockwaves, including (1) backward recovery, (2) ideal forward recovery, (3) ideal backward forming, (4) backward forming, and (5) forward recovery, are introduced. In common with existing literatures, a shockwave with the term *forward* indicates the propagation direction of it the same as vehicle trajectory and with the term *backward* indicating that in opposite to vehicle trajectory. The estimation method of upstream speed and flow is discussed in Section 2.4. An algorithm, which detects shockwaves with traffic parameters, is demonstrated in Section 2.5. However, this study still assumes (1) no heavily spillover from downstream resulted in the residual queue beyond detection zone, and (2) no incident occurs. The first assumption pertains to the discussed shockwave structure with reasonable formation and discharging processes. It is pertinent to most cases of oversaturation but only the case with the residual queue over detection zone.

2.1. Relations between shockwaves and the assumed asymmetric fundamental diagram

This subsection gives a preliminary illustration of the discussed shockwave structure and flow-density curve. The notations employed here would be favorable throughout this paper. Since the backward moving shockwaves are much slower than the forward moving shockwaves, this study utilizes an asymmetric fundamental diagram of flow-density curve composed of a parabolic function before reaching maximal flow state, Q_m, and then following a linear equation starting from Q_m and halting at jam density, K_j. The proposed stream flow diagram is demonstrated in Fig. 2. Let flow, density, and speed under flow state x (ⓧ in Fig. 2) be denoted as Q_x, K_x, and U_x, respectively. The flow state 0 (⓪ in Fig. 2) is defined as the state of jam density K_j; while the flow state 1 (① in Fig. 2) is defined as the state which has the maximal flow rate Q_m and density K_m. The maximal flow rate Q_m also represents the saturation flow rate of green phase at a signalized intersection. With proposed flow model, we have $Q_0 = 0$ and $K_j = aK_m$, where a is a constant needs to be calibrated. If the real traffic flow can be represented as the Greenshields' model, which is symmetric on both non-congested and congested part, the constant a equals 2. Since backward moving shockwaves are much slower than forward moving shockwaves, the constant a should be greater than 2. For example, with the asymmetric Greenberg's model, the constant a is equal to nature base of logarithms e (2.718).

With a flow state x, the speed of shockwaves among different states can be graphically seen in Fig. 2; while W_{01} denotes the shockwave between state 1 and 0, W_{x1} is the shockwave between state x and 1, and W_{x0} is the shockwave between state x and 0. Throughout this article, W represents the shockwave speed.The W_{01} can be calculated as

$$W_{01} = \frac{Q_0 - Q_1}{K_0 - K_1} = \frac{-Q_m}{(a-1)K_m}. \tag{1}$$

The W_{x0} and W_{x1} can be calculated as some ratio of the W_{01} by using the following equations.

$$W_{x1} = \frac{Q_x - Q_1}{K_x - K_1} = \sqrt{1-r}\frac{Q_m}{K_m} = (1-a)\sqrt{1-r}W_{01}, \tag{2}$$

$$W_{x0} = \frac{Q_x - Q_0}{K_x - K_0} = \frac{rQ_m}{(1-a-\sqrt{1-r})K_m} = \frac{r(1-a)}{(1-a-\sqrt{1-r})}W_{01}, \tag{3}$$

where r is the flow ratio between Q_x and Q_m, $Q_x = rQ_m$.

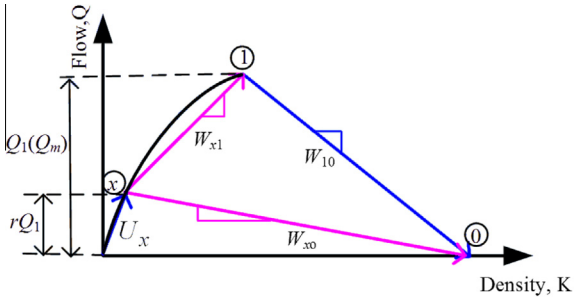

Fig. 2. The relation between shockwaves.

With the above equations, we have the relation among W_{x0}, W_{x1} and W_{01}, which follows

$$W_{x1} = \frac{1}{2}\left(W_{x0} + W_{01}\sqrt{\left(\frac{W_{x0}}{W_{01}}\right)^2 - 4(1-a)^2\frac{W_{x0}}{W_{01}} + 4(1-a)^2}\right). \tag{4}$$

By using a Taylor series expansion, W_{x1} can be approximated as

$$W_{x1} = \frac{1}{2}(aW_{x0} + 2(1-a)W_{01}). \tag{5}$$

After deriving W_{x0}, W_{x1} and W_{01}, the flow ratio r between Q_x and Q_m can be calculated as

$$r = \frac{W_{x0}\sqrt{4(a-1)^2W_{01}^2 - 4(a-1)^2W_{01}W_{x0} + W_{x0}^2} + 2(a-1)^2W_{01}W_{x0} - W_{x0}^2}{2(a-1)^2W_{01}^2}. \tag{6}$$

Therefore, the corresponding space mean speed U_x and flow rate Q_x can be calculated as

$$U_x = (1-a)(1+\sqrt{1-r})W_{01} \tag{7}$$

$$Q_x = \frac{W_{x0}\sqrt{4(a-1)^2W_{01}^2 - 4(a-1)^2W_{01}W_{x0} + W_{x0}^2} + 2(a-1)^2W_{01}W_{x0} - W_{x0}^2}{2(a-1)^2W_{01}^2}Q_m \tag{8}$$

From Eq. (1) to (8), we found that all the shockwave speeds and the volume and the space mean speed for upstream traffics can be expressed as a function of W_{01}, W_{x0}, and the parameter a.

2.2. Traffic parameters: stopped duration, moving duration and empty duration

This subsection introduces the definition of traffic parameters including stopped duration, moving duration, and empty duration. A typical time–space diagram of signalized intersection is shown in Fig. 3, with the vehicle trajectory is indicated as black lines. The traffic parameter, stopped duration, is defined as the vehicle presence at detection zone for an extensive period (for example, 3 s for cars and 10 s for trucks) of time; while moving duration is defined as the vehicle presence less than that period. The parameter, empty duration, represents no vehicle presence at that period. To improve accuracy, multiple detectors can be used to check whether a vehicle is stopped or not. The stopped duration can also be obtained when the speed equals zero.

2.3. Detection of shockwaves for signalized intersection

This subsection introduces the estimation of shockwave from vehicle detector data. The shockwaves for a signalized intersection is shown in Fig. 4. Gray lines represent the trajectories of individual vehicles, while black lines or black dash lines indicate shockwaves. This study defines four dedicated flow states. First, flow state 0 (⓪ in Fig. 4) represents a traffic state with maximal density and the speed equals zero. Second, the flow state 1 (① in Fig. 4) represents the maximum flow state (defined as flow equals saturated flow rate). Third, flow state 2 (② in Fig. 4) is defined as the ideal traffic flow, which means vehicles arrive within a cycle equals the saturation flow of green phase. Fourth, flow state 3 (③ in Fig. 4) is defined as the uniformly distributed flow over a cycle, which might be different from cycle to cycle.

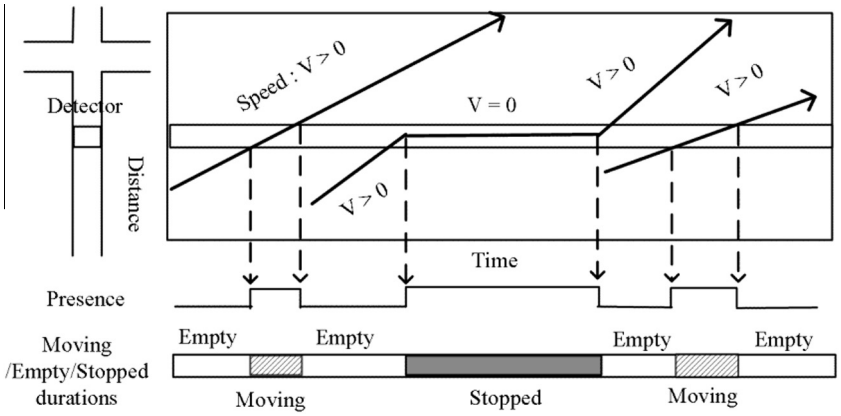

Fig. 3. The demonstration of traffic parameters: moving duration, empty duration and stopped duration.

There are three shockwaves among states 0, 1, and 2; W_{20} is defined as ideal backward forming shockwave, W_{21} is defined as ideal forward recovery shockwave, and W_{01} represents a backward recovery shockwave. Fig. 4(b) demonstrates a similar situation as Fig. 4(a) but with higher arrival rate (as state 3). Among state 0, 1, and 3, we have shockwaves of (1) W_{30}, a backward forming shockwave, (2) W_{31}, forward recovery shockwave, and (3) W_{01}, a backward recovery shockwave. Moreover, it can be observed in Fig. 4(b), where state 3 has a higher arrival rate than state 2, the propagation speed of shockwaves W_{30} would be greater than W_{20} and the speed of W_{31} would be slower than W_{21}. Fig. 4(c) and (d) show the relationships among five shockwaves on the fundamental diagram and the time–space diagram.

The rest of the subsection would describe the shockwave detection method via traffic parameters including stopped duration, moving duration, and empty duration.

2.3.1. Back ward recovery shockwaves detection

When the signal changes to green, a backward recovery shockwave W_{01} is formed between stopped vehicles and the vehicles start to move forward. If the vehicle stopped on the detection zone of vehicle detector starts to move after time; Let ΔT be the time difference between the time that green phase begins and the time that state of vehicle detector changes from stopped duration to moving duration (see Fig. 5). Following the concept proposed by May [14], the backward recovery shockwave can be calculated by,

$$W_{01} = -\frac{D}{\Delta T} \tag{9}$$

where D is the distance from stop line to the location of detector.

2.3.2. Ideal forward recovery and backward forming shockwaves calculation

To calculate the shockwaves in an intersection, this study introduces two *ideal* shockwaves; one is the *ideal forward recovery shockwave*, the other is the *ideal backward shockwave*. The ideal forward recovery shockwave is formed at where the ideal arrival traffic flow that catches the forward moving saturation flow; the shockwave can be graphically shown as the boundary between state 2 and 1 in Fig. 4.

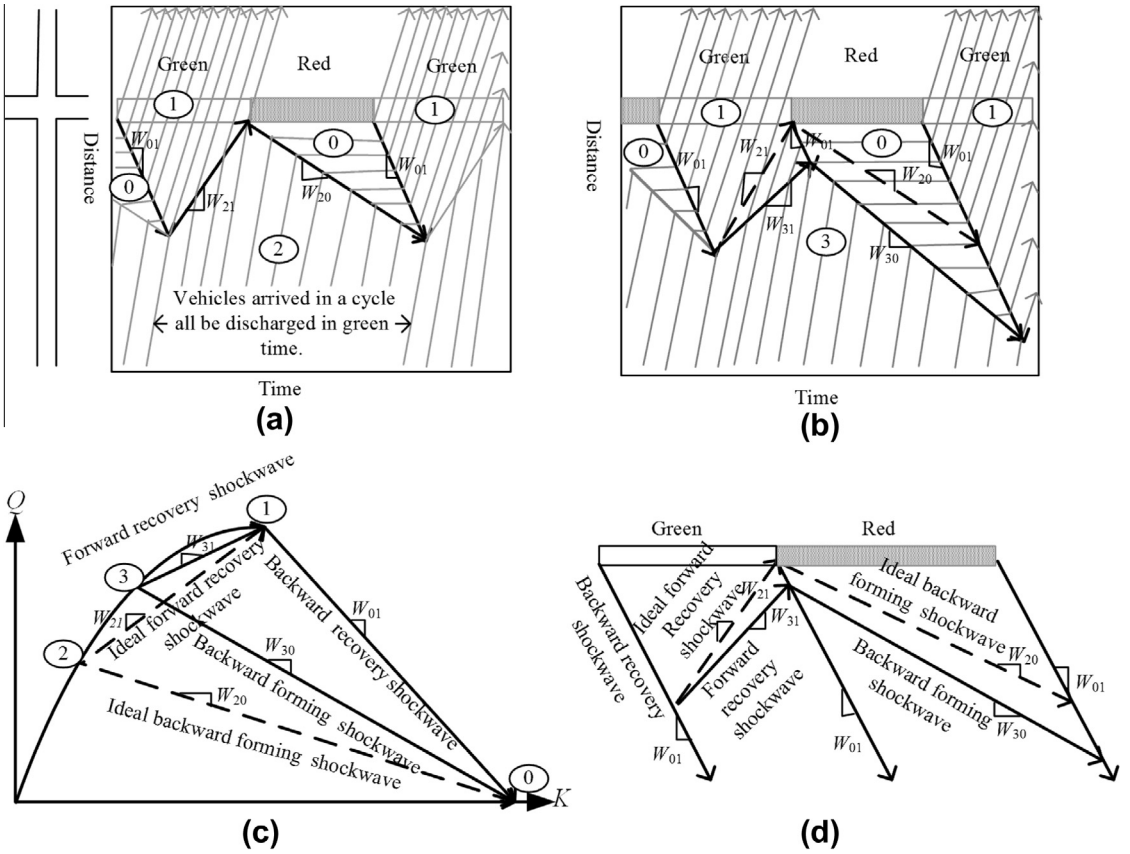

Fig. 4. (a) Ideal shockwaves for a specified green and red time, (b) comparison between the ideal shockwaves and general shockwaves, (c) five shockwave relations in the proposed model, (d) five shockwave relations in time–space diagram.

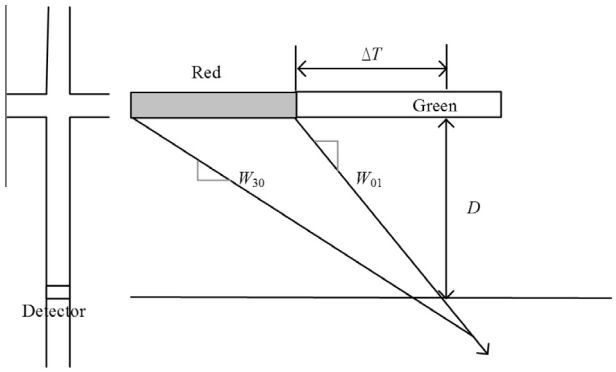

Fig. 5. Backward recovery shockwave detection.

The ideal flow rate, Q_2, can be calculated through green split of a signal cycle (g/c) and saturation flow rate (Q_m).

$$Q_2 = g/c\,Q_m = rQ_m \tag{10}$$

The flow ratio r between Q_2 and Q_m is equal to g/c. To replace x with 2 in Eq. (2), the ideal forward recovery shockwave can be calculated as,

$$W_{21} = (1-a)\sqrt{1-g/c}\,W_{01}. \tag{11}$$

Similarly, to replace x with 2 in Eq. (3), the ideal backward forming shockwave can be calculated as,

$$W_{20} = \frac{g/c(1-a)}{(1-a-\sqrt{1-g/c})}W_{01}. \tag{12}$$

The equations above show that the ideal shockwaves, W_{21} and W_{20}, can be simplified to a ratio of the backward recovery shockwave W_{01}. Therefore, with backward recovery shockwave W_{01}, green split and calibrated constant a, the ideal shockwaves can be calculated by Eqs. (11) and (12).

2.3.3. Backward forming shockwaves detection

This subsection discusses the calculation of a backward forming shockwave. The calculation method can be categorized into two types: (1) the method which utilizes moving and empty duration, and (2) the calculation method which utilizes stopped duration. Parameters of moving duration and empty duration are generated from the detector while there are no stopped vehicles within the detection area; otherwise, the parameter of stopped duration is outputted.

2.3.3.1. Using moving duration and empty duration for general backward forming shockwave detection. Before the traffic queue reaches the detector, the sensor would output moving duration and empty duration. The time–space relations among backward forming shockwave, moving duration and empty duration, are illustrated in Fig. 6. The speed of the first vehicle and the speed of the nth vehicle are both approximated by the space mean speed of the n passing vehicles observed at detection zone. As vehicle i, $i = 1, \ldots, n$, with speed u_i and length L_i passes a detecting zone with length L_z, this will result a moving duration m_i equal to $(L_i + L_z)/u_i$. As no vehicle within the detecting zone, it will result an empty duration e_i. Let E be the summation of all empty durations e_i and M be the summation of all moving duration m_i during a time interval ΔT. Assume the length of detecting zone be approximately the same as the gap between two stopped vehicles, then the summation of moving duration M can be calculated as the following equation,

$$M = \sum_{i=1}^{n} m_i = \sum_{i=1}^{n} \frac{(L_z + L_i)}{u_i} \cong \sum_{i=1}^{n} \frac{(L_z + \bar{L})}{u_i} = \frac{L_q}{u_s} = \Delta t, \tag{13}$$

where L_q denotes the queue length resulting from the vehicles during time interval ΔT, $\bar{L}$ the average vehicle length of the n vehicles, u_s the space mean speed of the n vehicles observed at detection zone, and Δt is the time interval shown in Fig. 6. According the geometry relations in Fig. 6, the summation of all empty duration E can be calculated as

$$E = \Delta T - M \approx \Delta T - \Delta t. \tag{14}$$

Moreover, the geometry relationship also leads to the following backward forming shockwave equation.

$$W_{30} = -\frac{L_q}{\Delta T - \Delta t} \approx -\frac{L_q}{E} = -\frac{Mu_s}{E} \tag{15}$$

The backward forming shockwave can be calculated using Eq. (15) with the parameters of vehicle speed (V), moving duration (M), and empty duration (E).

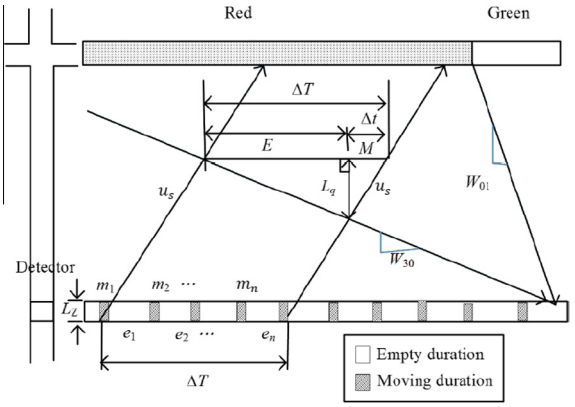

Fig. 6. Relation among backward forming shockwave, moving duration and empty duration.

2.3.3.2. Using stopped duration for backward forming shockwave detection. After the queue reaches the detector during red phase, stopped duration would be used for shockwave calculation. Figs. 7 and 8 illustrate the changes in the stopped duration for two consecutive signal cycles which have same red phase duration. Fig. 7 demonstrates the case which the propagation speed of backward forming shockwave is greater than the ideal backward forming shockwave. It should be noted that since the propagation direction of backward forming shockwave is opposite to vehicle trajectory, the term *greater* actually means the absolute value of W_{30} is greater than the absolute value of W_{20}. In this case, the stopped duration is increasing for two consecutive cycles.

On the contrary, Fig. 8 shows the case which the propagation speed of backward forming shockwave is less than the ideal backward forming shockwave. The stopped duration in this case is decreasing for two consecutive cycles. Since the two cases resemble each other, the following analyses and equations can be applied to both cases.

The stopped duration of the first cycle is $\overline{O_1A_1}$, while that of the second cycle is $\overline{O_2C_2}$. $\overline{O_1A_1}$ is almost equal to $\overline{O_2A_2}$ if the traffic flow changes smoothly. Hence, the stopped duration difference for these two consecutive cycles is $\overline{A_2C_2}$, or ΔS_C. Since the dashed lines have the same slope as the shockwave W_{30}, $\overline{AC}$ is equal to $\overline{A_2C_2}$. $\overline{AC}$ is the sum of $\overline{AB}$ and $\overline{BC}$. $\overline{AB}$ has the same length as ΔS_R and $\overline{BC}$ has the same length as ΔS_G. $\overline{BC}$, or ΔS_G, is derived from the flow difference between shockwaves W_{21} and W_{31} during the green phase G. $\overline{AB}$, or ΔS_R, can be calculated from the flow difference between shockwaves W_{20} and W_{30} during the red phase R.Therefore,

$$\Delta S_C = \Delta S_G + \Delta S_R \tag{16}$$

To calculate ΔS_R, we should consider Fig. 7(b) and (c). Let a Euclidean space represents the time–space diagram of Fig. 7(c) and set point A to be (0, 0). In this case, the shockwave propagation speed, W, is acted as slope. By using linear algebra, point E can be obtained from lines AE and DE,

$$E(X_E, Y_E): \begin{cases} \overleftrightarrow{AE}: Y = W_{20}X \\ \overleftrightarrow{DE}: Y = W_{01}(X + R) \end{cases} \tag{17}$$

Furthermore, point B can be derived from lines AB and BE,

$$B\left(\frac{RW_{01}(W_{20} - W_{30})}{W_{30}(W_{01} - W_{20})}, 0\right): \begin{cases} \overleftrightarrow{AB}: Y = 0 \\ \overleftrightarrow{BE}: Y - Y_E = W_{30}(X - X_E) \end{cases} \tag{18}$$

Hence

$$\Delta S_R = \overline{AB} = \frac{RW_{01}(W_{20} - W_{30})}{W_{30}(W_{01} - W_{20})} \tag{19}$$

Similarly, ΔS_G can be calculated from the flow difference between shockwave W_{21} and W_{31} during the green phase G. To calculate ΔS_G, we should consider Fig. 7(b) and (d). Let a Euclidean space represents the time–space diagram of Fig. 7(d) and set point I to be (0, 0). The point E can then be obtained from lines IE and JE using linear algebra

$$E\left(\frac{GW_{01}}{W_{01} - W_{21}}, \frac{GW_{01}W_{21}}{W_{01} - W_{21}}\right): \begin{cases} \overleftrightarrow{IE}: Y = W_{21}X \\ \overleftrightarrow{JE}: Y = W_{01}(X - G) \end{cases} \tag{20}$$

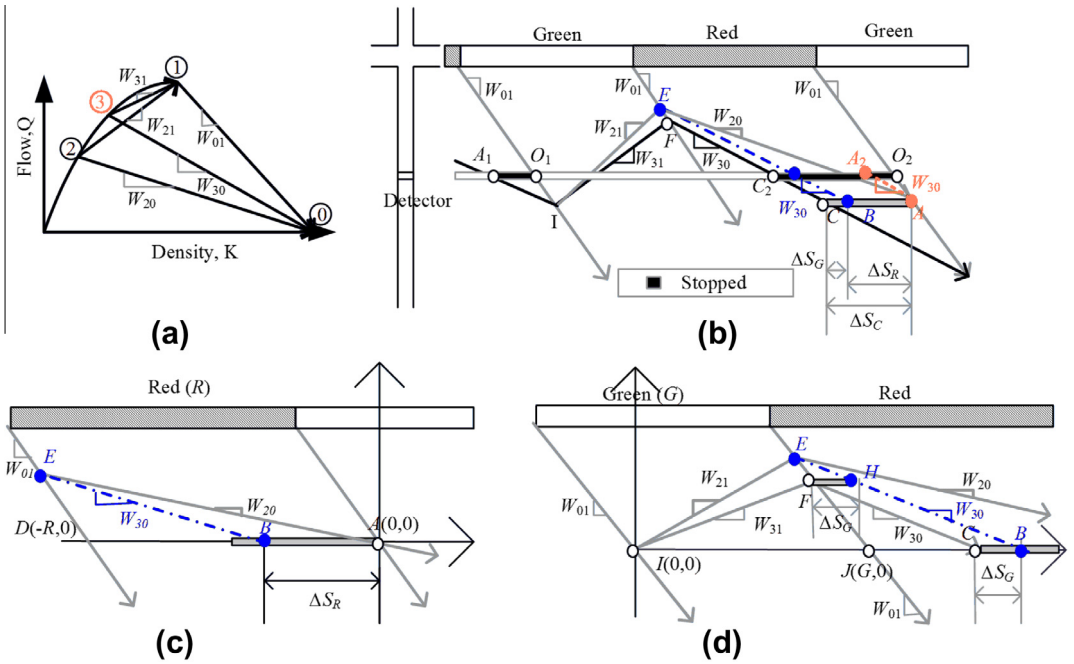

Fig. 7. Case for backward forming shockwave $|W_{30}| > |W_{20}|$ (a) shockwaves in flow-density diagram, (b) shockwave and incremental stopped duration, (c) incremental stopped duration in red phase, (d) incremental stopped duration in green phase.

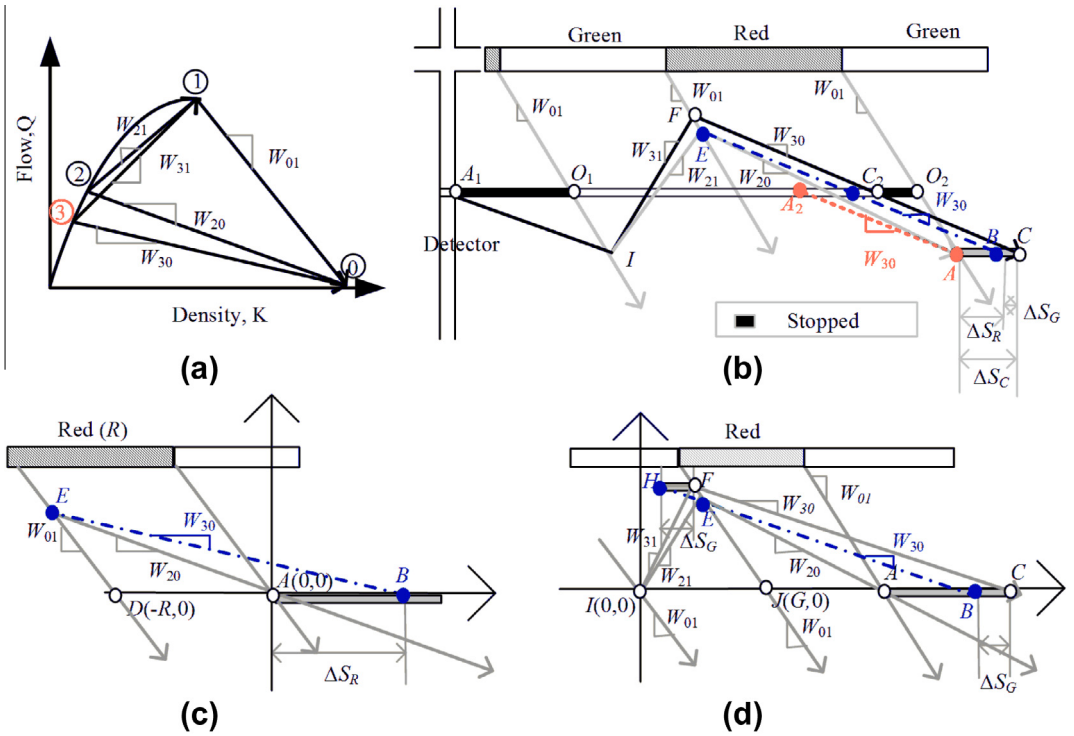

Fig. 8. Case for backward forming shockwave $|W_{30}| < |W_{20}|$ (a) shockwaves in flow-density diagram, (b) shockwave and reductive stopped duration, (c) reductive stopped duration in red phase, (d) reductive stopped duration in green phase.

Also point F can be derived from lines IF and JF,

$$F\left(\frac{GW_{01}}{W_{01}-W_{31}},\frac{GW_{01}W_{31}}{W_{01}-W_{31}}\right):\begin{cases}\overleftrightarrow{IF}: Y = W_{31}X\\ \overleftrightarrow{JF}: Y = W_{01}(X-G)\end{cases} \tag{21}$$

And point H can be calculated from lines FH and EH,

$$H(X_H,Y_H):\begin{cases}\overleftrightarrow{FH}: Y = Y_F\\ \overleftrightarrow{EH}: Y - Y_E = W_{30}(X-X_E)\end{cases} \tag{22}$$

Therefore

$$\Delta S_G = \overline{BC} = \overline{FH} = \frac{GW_{01}(W_{01}-W_{30})(W_{31}-W_{21})}{W_{30}(W_{01}-W_{21})(W_{01}-W_{31})} \tag{23}$$

Replace x by 3 in Eq. (3), we would have the following equation,

$$W_{31} = \frac{1}{2}(aW_{30} + 2(1-a)W_{01}) \tag{24}$$

Substitute W_{21} and W_{31} in Eq. (23) by Eqs. (12) and (24),

$$\Delta S_G = \frac{GW_{01}(W_{01}-W_{30})(W_{30}-W_{20})}{W_{30}(W_{01}-W_{21})(2W_{01}-W_{30})} \tag{25}$$

Therefore, ΔS_C can be calculated by

$$\Delta S_C = \Delta S_G + \Delta S_R = \frac{GW_{01}(W_{01}-W_{30})(W_{30}-W_{20})}{W_{30}(W_{01}-W_{21})(2W_{01}-W_{30})} + \frac{RW_{01}(W_{20}-W_{30})}{W_{30}(W_{01}-W_{20})} \tag{26}$$

The calculation of shockwaves with parameter of stopped duration, the following procedure can be applied. We have the red phase duration R and green phase duration G given by traffic controller; and the backward recovery shockwave W_{01} calculated by Eq. (9). When there is no spillover, the speed of shockwave W_{01} is nearly constant. The ideal shockwaves, W_{20} and W_{21}, can be calculated from Eqs. (11) and (12) with given R and G. Therefore, the stopped duration differences, ΔS_G, can immediately be calculated after detecting a stopped vehicle. After deriving stopped duration difference, from vehicle detection, the backward forming shockwave W_{30} can be calculated by Eq. (26). The calculating procedure can be applied to Fig. 8 and having the same result.

If the red phase duration (R) is not fixed for two consecutive cycles, then Eq. (26) must be modified as,

$$\Delta S_C = \Delta S_G + \Delta S_R + \Delta R = \frac{GW_{10}(W_{10}-W_{30})(W_{30}-W_{20})}{W_{30}(W_{10}-W_{21})(2W_{10}-W_{30})} + \frac{RW_{10}(W_{20}-W_{30})}{W_{30}(W_{10}-W_{20})} + \Delta R \tag{27}$$

where ΔR is the red phase duration difference of two consecutive cycles.

2.3.3.3. Backward forming shockwave detection under heavy congestion. If the queue has the length more than the vehicle detector installation location plus the length of queue that can be discharged during green phase, it would cause the detector to output the traffic parameter of stopped duration be the same as red phase duration, as Fig. 9. In this case, Eqs. (26) and (27) cannot be used to calculate the backward forming shockwave. Additional vehicle detectors can be added to solve this problem; the Eqs. (26) and (27) can be applied to new detectors. If the installation of new detector is not possible, the moving average, as Eq. (28), can be used to predict the backward forming shockwave.

$$W_{30}(n) = \frac{1}{5}W_{30}(n-1) + \frac{1}{5}W_{30}(n-2) + \frac{1}{5}W_{30}(n-3) + \frac{1}{5}W_{30}(n-4) + \frac{1}{5}W_{30}(n-5) \tag{28}$$

where $W_{30}(n)$ is current shockwave value, $W_{30}(n-i)$ is the i-th previous shockwave value.

2.3.4. Forward recovery shockwave detection

The forward recovery shockwave can easily be calculated using Eq. (24). In general, the backward recovery shockwave W_{01} is calculated first, followed by the backward forming shockwave W_{30}. The forward recovery shockwave, W_{31}, is the last shockwave to be calculated. Therefore, the shockwaves can be derived right after the detection of stopped vehicle. Compare to existing researches, which the shockwaves can only be derived after the beginning of green time; the proposed method can support real-time application.

2.4. Upstream speed and flow detection

This sub-section focuses on the estimation of upstream speed and flow. The upstream means the state which is not affected by the queue; state 3 is a common representative. If all shockwaves of state 3 are derived, the arrival flow rate can be calculated by Eqs. (6) and (8). Replace x with 3 in Eq. (6), the arrival flow ratio r is

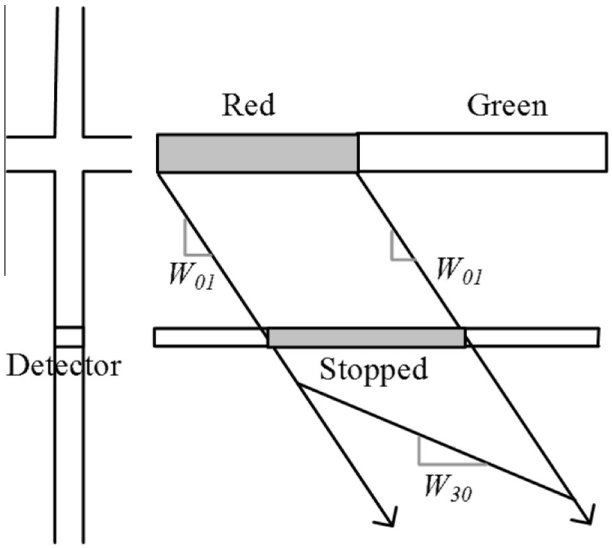

Fig. 9. A vehicle's stopped duration is equal to the red phase time.

$$r = \frac{W_{30}\sqrt{4(a-1)^2W_{01}^2 - 4(a-1)^2W_{01}W_{30} + W_{30}^2} + 2(a-1)^2W_{01}W_{30} - W_{30}^2}{2(a-1)^2W_{01}^2} \tag{29}$$

The flow is calculated as the following equation,

$$Q_3 = rQ_m = \frac{W_{30}\sqrt{4(a-1)^2W_{01}^2 - 4(a-1)^2W_{01}W_{30} + W_{30}^2} + 2(a-1)^2W_{01}W_{30} - W_{30}^2}{2(a-1)^2W_{01}^2}Q_m \tag{30}$$

where Q_m is the saturation flow rate, which can be investigated in advance. The speed of state 3 can be derived from Eq. (6),

$$U_3 = \frac{(1-a)r}{1-\sqrt{1-r}}W_{01} \tag{31}$$

where U_3 represents the space mean speed of state 3.

2.5. Proposed algorithm

This section proposes an algorithm to calculate shockwaves that being discussed in the Section 2.3. The proposed algorithm is demonstrated as Fig. 10(a). First, gather presence data from vehicle detector; second, calculate traffic parameters including empty duration, moving duration, and stopped duration. Third, the calculation of backward recovery shockwave and followed by fourth, the calculation of ideal shockwaves. Fifth, backward forming shockwave is calculated. Last, forward recovery shockwave is obtained. The estimation method of backward forming shockwave is detailed in Fig. 10(b). This figure demonstrates the usage of multiple detectors to predict backward forming shockwave; although the figure illustrates the procedure by two detectors, it can be easily extended to multiple detectors. The first step is setting a vehicle detector near the stop line and the other at the upstream. The spacing between detectors should be more than the length of queue that can be discharged during maximal green time. If the first detector do not gives a stopped duration, then the moving duration and empty duration of first detector is utilized in the calculation of backward forming shockwave. Otherwise, stopped duration is taken into consideration. Moreover, if the stopped duration is larger than red time, the next detector should be considered; the above procedure should be repeated again for the next detector. The whole procedure ends at the last detector. If all detectors have the stopped durations as red time, estimation method of Eq. (28) should be used.

3. Simulation results

A CORSIM simulation environment has been established to evaluate the traffic parameters and the proposed shockwave detection methods. An independent intersection with four approaches is created in the CORSIM environment. Two vehicle sensors are located 300 and 730 feet from the stop line on an approach, as Fig. 11 shows. Fig. 12 illustrates the phase time and input traffic flow of that approach. During the simulation, the headway distribution is set to be uniform, and the traffic is

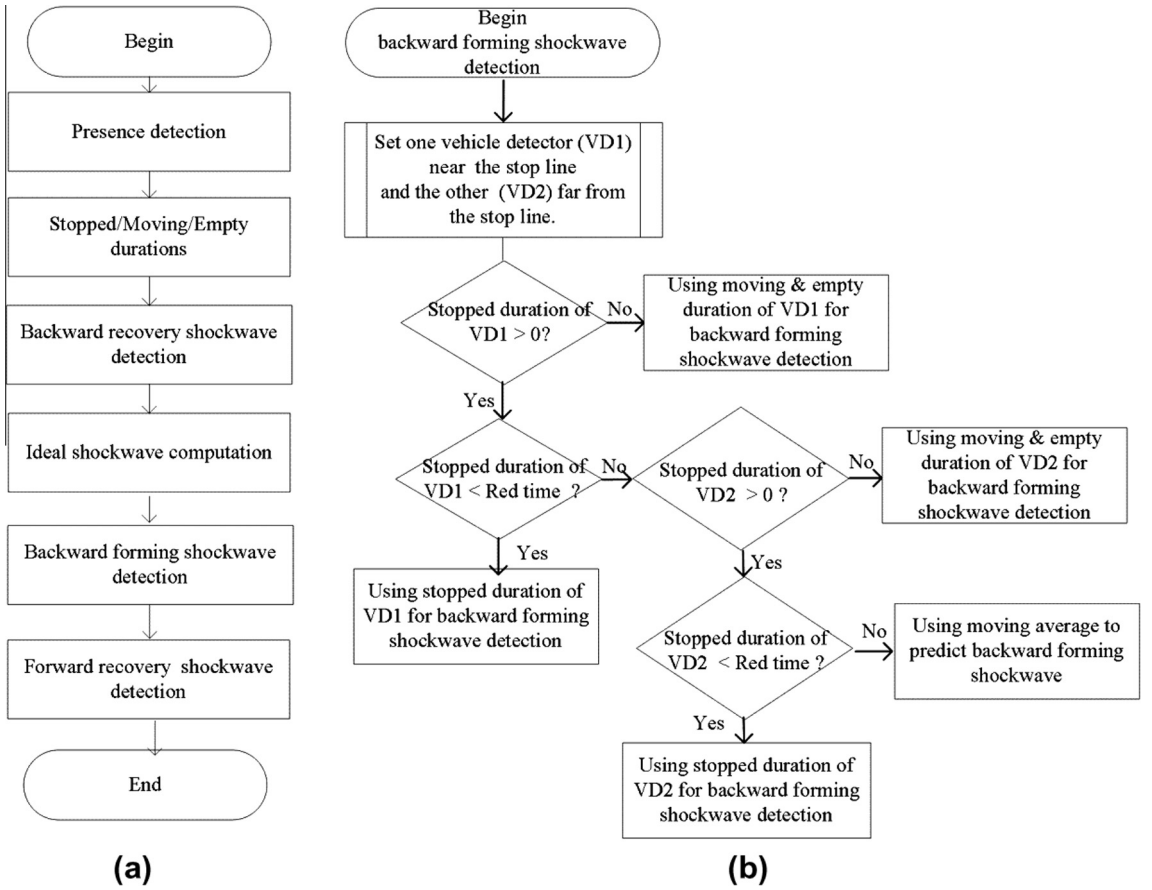

Fig. 10. (a) The algorithm for five shockwaves detection, (b) the algorithm for backward forming shockwave detection.

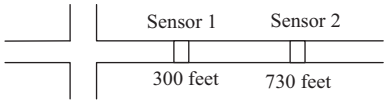

Fig. 11. The intersection of simulation: a link and two sensors' locations.

only comprised of passenger cars. No spillover occurs during the simulation period; therefore, all stopped vehicles are caused by red signals. This simulation is a sample intersection near ramp of highway or freeway in rush hours. To demonstrate the capability of the proposed method, the signal timing in this simulation is designed to be dynamically changed. The change of phase time may be resulting from some adaptive control methods; as the traffic flow increases, the green time also increases.

3.1. Traffic parameters

Fig. 13 shows the traffic parameters derived from both vehicle detectors during the simulation period. Due to changes in phase duration, some cycle length is shorter or longer than others are. With low traffic flow demands, both detectors output empty duration and moving duration. The stopped duration is only presented when traffic queue reaches the detecting zone. Fig. 14 compares the red phase duration and the stopped duration of both detectors. Notably, the stopped duration of both detectors approaches the red time, indicating that queue length of un-discharged vehicles reaches beyond the second detector. Moreover, since the first detector is installed closer to stop line than the second one, the first detector would always have more cycles that reports stopped duration.

3.2. Results of shockwaves

According to Section 2, each method of the backward forming shockwave is valid only for a specific circumstance. For example, Eq. (15) should be used when no stopped duration occurs, otherwise Eqs. (26) and (27) should be used instead.

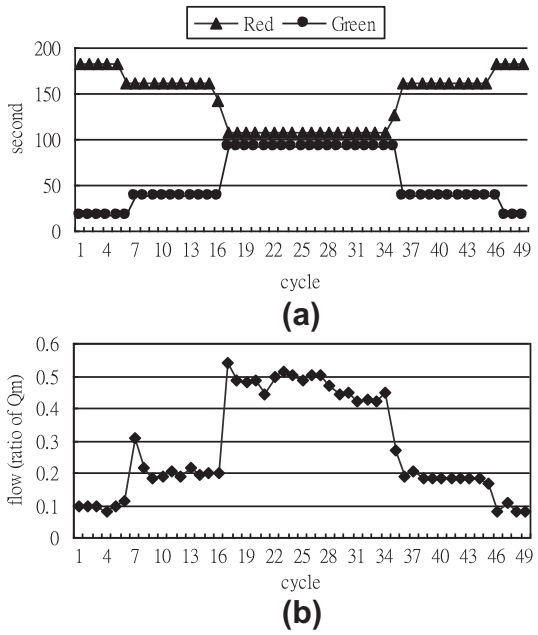

Fig. 12. (a) the phase times of the intersection, (b) the input flow of the link.

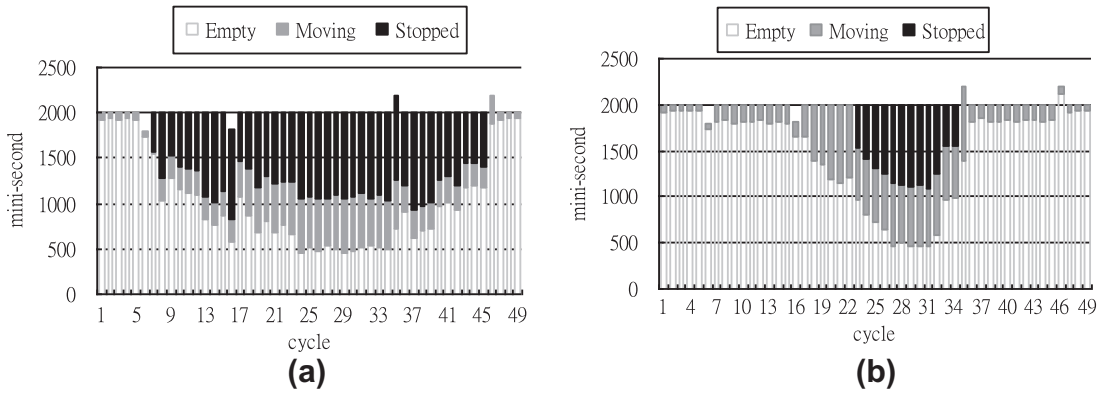

Fig. 13. (a) The stopped duration, moving duration and empty duration of detector 1, (b) the stopped duration, moving duration and empty duration of detector 2.

If the stopped duration be equal to red phase duration, Eq. (28) can be taken into consideration. The constant a in those equations is calibrated as 2.1. The algorithm proposed in Section 2.5 indicates the proper usage of each equation. Fig. 15 demonstrates the backward forming shockwave calculation of each method and the final result of the proposed algorithm. In Fig. 15, $\triangle Si$ represents the tenth of the stopped duration difference of detector i for two consecutive cycles; while $S{-}i$, $M/E{-}i$, and $Mavg$ denote the shockwave calculated from stopped duration, moving/empty duration, and moving average, respectively. The calculated backward forming shockwave from the proposed algorithm is denoted as W_{30}. It can be observed in Fig. 15 that the speed of backward forming shockwave is negatively related to the stopped duration difference. As the stopped duration difference decrease, the backward forming shockwave speed increase, vice versa. The condition should holds theoretically. However, with stochastic driving behavior, some non-ordinary driving behavior occurs near the vehicle detector on the 17th cycle of simulation. Therefore, the statement would be violated on the 17th cycle.

Fig. 16 compares the shockwave calculating result derived from detector with the one that directly measured from CORSIM. In Fig. 16, the ideal forward recovery/backward forming shockwave is denoted as W_{21}/W_{20}; while W_{31}/W_{30} denotes the calculated forward recovery/backward forming shockwave. The directly measured ones are denoted as W^*_{31} and W^*_{30}, respectively. In Fig. 16, the calculated shockwaves are similar to the directly measured ones, which represent a significant

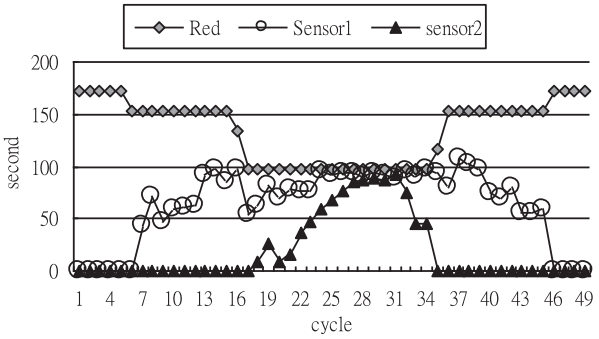

Fig. 14. Relation between the stopped duration and red phase time.

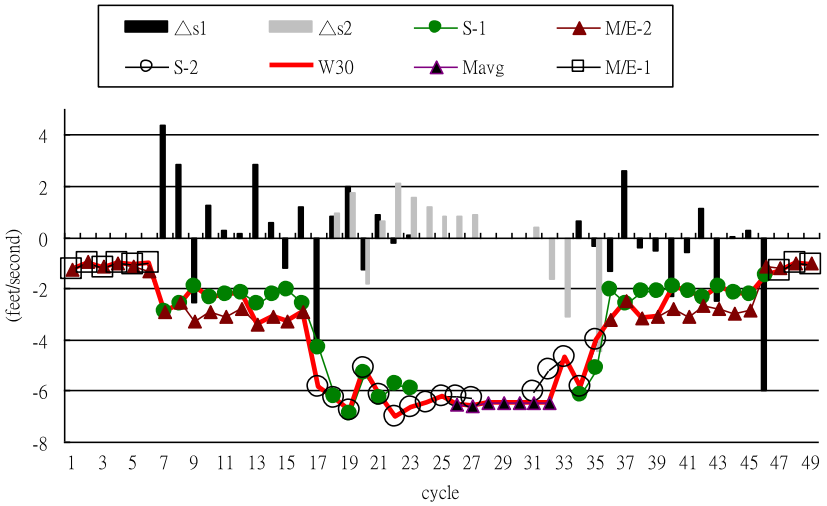

Fig. 15. Results of the backward forming shockwave detection algorithm.

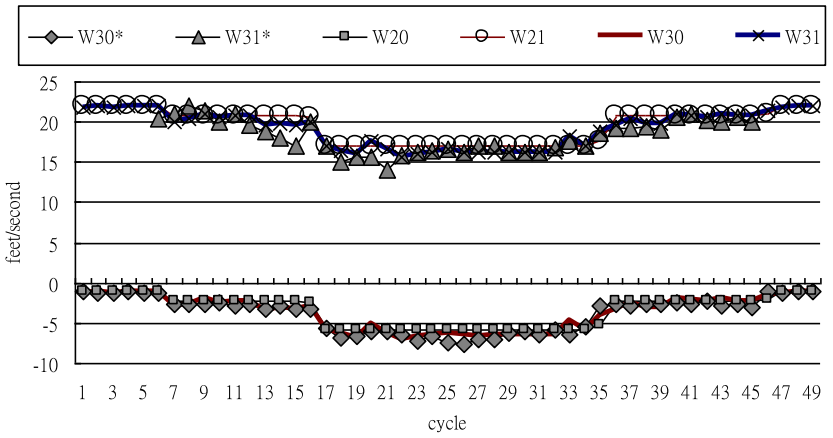

Fig. 16. Comparison of calculated / directly-measured shockwaves of the approach.

result. In the simulation, the intersection has a fixed saturation flow rate, without the disturbance from downstream spillover; therefore, W_{01} would maintain a stable value (−21 ft/s herein).

The mean absolute percentage error (MAPE) of W_{30} is 12.4% and the mean absolute error (MAE) is 0.42 ft/s. While the MAPE and MAE of W_{31} is 4% and 0.69 ft/s, respectively. The bias mainly comes from the vehicle arrival pattern; as the vehicle

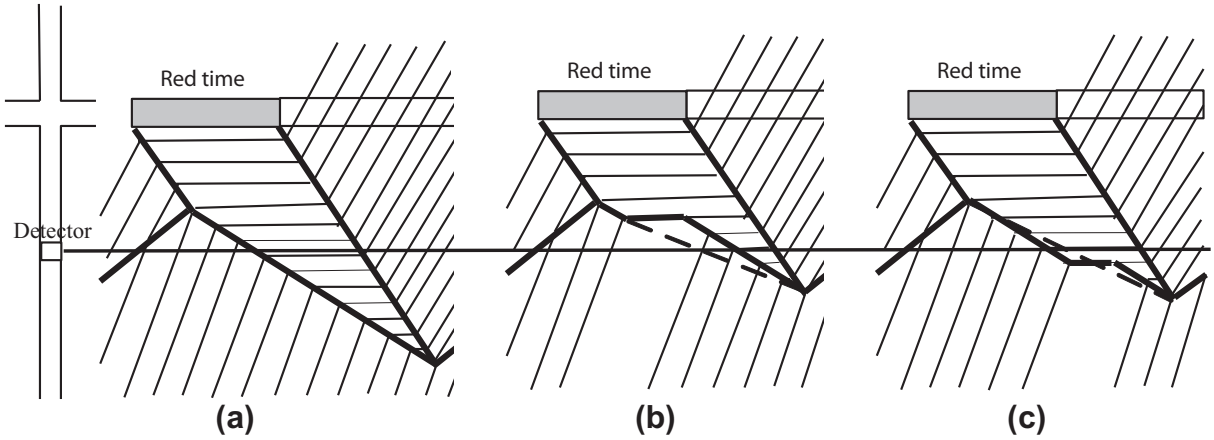

Fig. 17. The comparison of different arrival pattern and its corresponding bias in shockwave estimation, (a) uniform arrival pattern and its corresponding shockwave, (b) arrival pattern that gives an underestimated shockwave speed, and (c) arrival pattern that gives an overestimated shockwave speed.

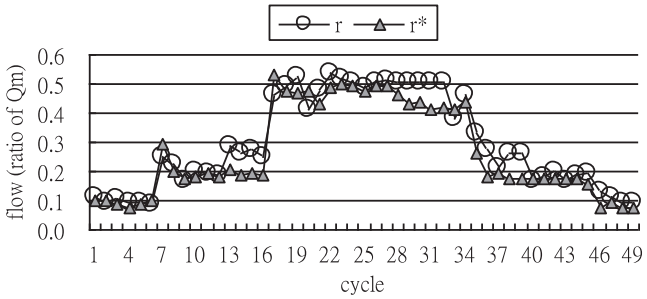

Fig. 18. The predicted traffic flow of state 3.

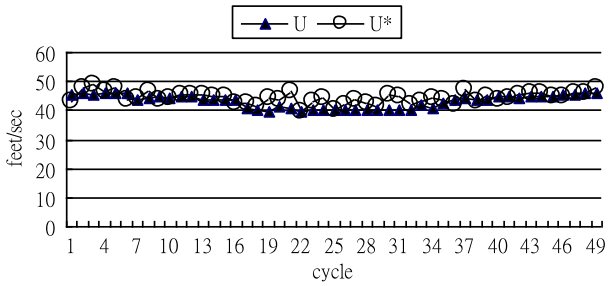

Fig. 19. The predicted traffic speed of state 3.

comes uniformly as Fig. 17(a), the detected stopped duration and corresponding shockwave detection would be unbiased. If vehicles arrive as platoons as shown in Fig. 17(b) or (c), the inaccurate stopped duration would result biased W_{30}. Fig. 17(b) demonstrates that, as the queue results from the first platoon does not reach detector and there exists a major gap between the first and the second platoon, the stopped duration would be underestimated. The underestimated stopped duration would result in a slower shockwave speed (indicated as dash line). Fig. 17(c) gives the counter example of overestimated stopped duration and the corresponding faster shockwave speed. During the simulation, it is observed that with more congested traffic; the less probability of major gap would happen.

3.3. Results of flow and speed

In Fig. 18, the estimated upstream flow is compared with the simulation input. To give a better understanding, these flow rates have been transformed into flow ratio (r). The flow ratio (r) is then compared with the flow ratio derived from

simulation (r^*). The comparison of estimated upstream speed (U) and detected speed (U^*) is illustrated in Fig. 19. The estimated upstream speed (U) is space mean speed but the detected speed is time mean speed; therefore, the detected speed is transformed to space mean speed with the method proposed by Drake, Schofer, and May (1967). The MAPE and MAE of flow ration are 18% and 0.03, respectively. While those of space mean speed are 4% and 1.79 ft/s, respectively. These results demonstrate that the proposed algorithm is capable of estimating flow and speed at upstream area.

4. Conclusions

In this paper, we proposed an innovative approach to estimate the upstream traffic information under oversaturated situation using shockwave analysis. A key methodological contribution of the approach is that it estimates shockwaves by combining traffic parameters, dynamic signal timing and traffic flow models. By utilizing parameters of stopped duration, moving duration, and empty duration, we are able to calculate shockwaves including (1) forward recovery, (2) ideal backward forming, (3) ideal forward recovery, (4) backward forming, and (5) forward recovery shockwave.

To the best of authors' knowledge, this is the first paper that utilizes real time shockwave by stopped duration to estimate upstream traffic flow and speed far beyond detection zones of vehicle detectors. With the shockwaves, upstream traffic flow and speed information can be estimated accordingly. These models are evaluated by traffic simulation and demonstrate a significant result. The proposed model has some pre-conditions for traffic flow state. These assumptions can be solved by combining linear regression and the information derived from multi-zone sensors to capture the variation of shockwaves.

Acknowledgements

The authors would like to thank the Ministry of Education of the Republic of China, Taiwan (MOE ATU Program), the National Science Council of the Republic of China, Taiwan (Contract No. NSC-95-2221-E-009-346, NSC-95-2221-E-009-347 and NSC-95-2752-E-009-010-PAE), and the Ministry of Transportation and Communications of the Republic of China, Taiwan (Contract No. MOTC-STAO-101-02) for financially supporting this research.

References

[1] G. Abu-Lebdeh, R.F. Benekohal, Development of traffic control and queue management procedures for oversaturated arterials, Transp. Res. Rec. 1603 (1997) 119–127.
[2] H.-J. Cho, S.C. Lo, Modeling of self-consistent multi-class dynamic traffic flow model, Phys. A 312 (2002) 342–362.
[3] H.-J. Cho, M.-T. Tseng, A novel computational algorithm for traffic control SoC, WSEAS Trans. Math. 5 (2006) 123–128.
[4] H.-J. Cho, M.-T. Tseng, Shockwave detection for electronic vehicle detectors, Lect. Notes Comput. Sci. 4490 (2007) 275–282.
[5] F. Dion, H. Rakha, Y.-S. Kang, Comparison of delay estimates at under-saturated and over-saturated pre-timed signalized intersections, Transp. Res. B 38 (2004) 99–122.
[6] N. Gartner, C.J. Messer, A.K. Rathi (Eds.), Traffic Flow Theory a State-of-the-Art Report Revisited, Organized by the Committee on Traffic Flow Theory and Characteristics (AHB45), Transportation Research Board, 2001
[7] D.C. Gazis, Traffic Theory, Kluwer Academic Publishers, Boston, 2002.
[8] D.C. Gazis, The origins of traffic theory, Oper. Res. 50 (2002) 69–77.
[9] D.L. Gerlough, M.J. Huber, Traffic Flow Theory: A Monograph, Transportation Research Board, 1975.
[10] B.D. Greenshields, A study of traffic capacity, in: Proceedings of the Highway Research Board, vol. 14, (1934) pp. 448–477.
[11] W. Leutzbach, Introduction to the Theory of Traffic Flow, Springer-Verlag, Berlin, 1988.
[12] M.J. Lighthill, G.B. Whitham, On kinematic waves: II. A theory of traffic flow on long crowded road, Proc. R. Soc. A 229 (1178) (1955) 317–345.
[13] H. Liu, X. Wu, W. Ma, H. Hu, Real-time queue length estimation for congested signalized intersections, Transp. Res. Part C 17 (2009) 412–427.
[14] A.D. May, Traffic Flow Fundamentals, Prentice Hall, Englewood Cliffs, New Jersey, 1990. 07632.
[15] Gregory Stephanopoulos, P.G. Michalopoulos, George Stephanopoulos, Modelling and analysis of traffic queue dynamics at signalized intersections, Transp. Res. A 13 (1979) 295–307.
[16] P.G. Michalopoulos, G. Stephanopoulos, V.B. Pisharody, Modeling of traffic flow at signalized links, Transp. Sci. 14 (1) (1980) 9–41.
[17] P.G. Michalopoulos, Gregory. Stephanopoulos, George. Stephanopoulos, An application of shock wave theory to traffic signal control, Transp. Res. B 15 (1981) 35–51.
[18] P.J. Richards, Shock waves on the highway, Oper. Res. 4 (42) (1956) 51.
[19] A. Skabardonis, N. Geroliminis, Real-time monitoring and control on signalized arterials, J. Intell. Transp. Syst. 12 (2) (2008) 64–74.
[20] G.B. Whitham, Linear and Nonlinear Waves, John Wiley and Sons, New York, 1974.
[21] X. Wu, H.X. Liu, N. Geroliminis, An empirical analysis on the arterial fundamental diagram, Transp. Res. Part B 45 (1) (2011) 255–266.
[22] X. Wu, H. Liu, D. Gettman, Identification of oversaturated intersections using high-resolution traffic signal data, Transp. Res. Part C 18 (4) (2010) 626–638.
[23] X. Wu, H. Liu, A shockwave profile model for traffic flow on congested urban arterials, Transp. Res. Part B 45 (2011) 1768–1786.